Experimental Validation of a Multibody Model for a Vehicle Prototype and its Application to State Observers

Roland Pastorino

A thesis submitted for the degree of *Doctor Ingeniero Industrial*

June 25, 2012, Ferrol, Spain

1. Motivations
2. Vehicle field testing
3. Vehicle modeling and simulation environment
4. Validation results
5. State observers
6. Conclusions

Laboratorio de Ingeniería Mecánica (LIM).

Specialized in real–time simulations of rigid and flexible multibody systems

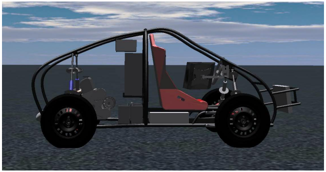

Fig. 1 – Real–time simulations of vehicles

Fig. 2 – Real–time simulations of excavators

Fig. 3 – Real–time simulations of container cranes

Fig. 4 – Human–In–The–Loop simulators of excavators

Multibody dynamics analysis in the automotive field.

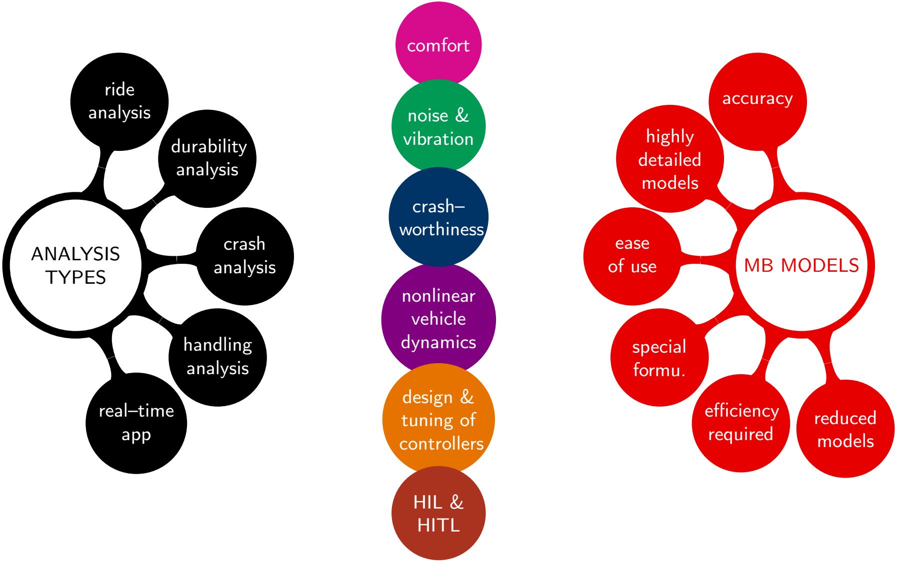

Multibody dynamics analysis in the automotive field.

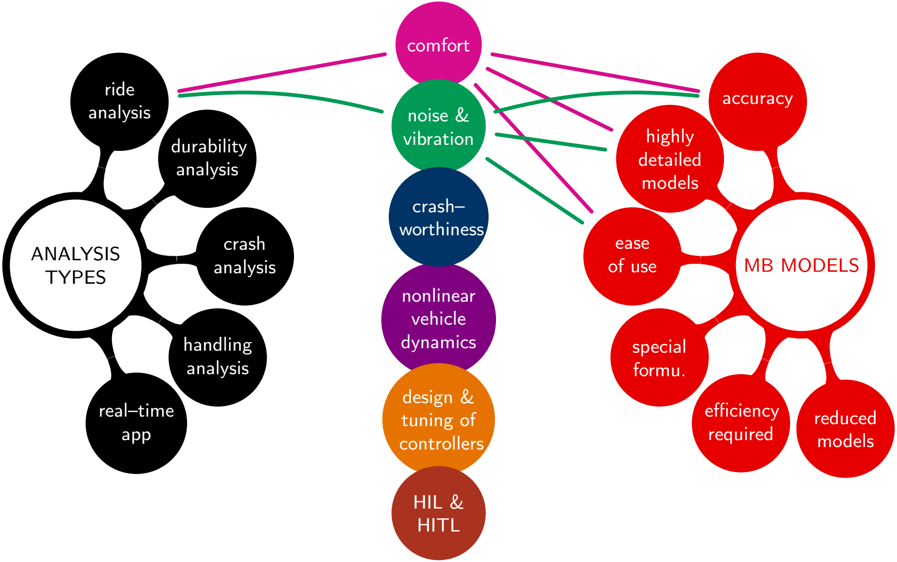

Multibody dynamics analysis in the automotive field.

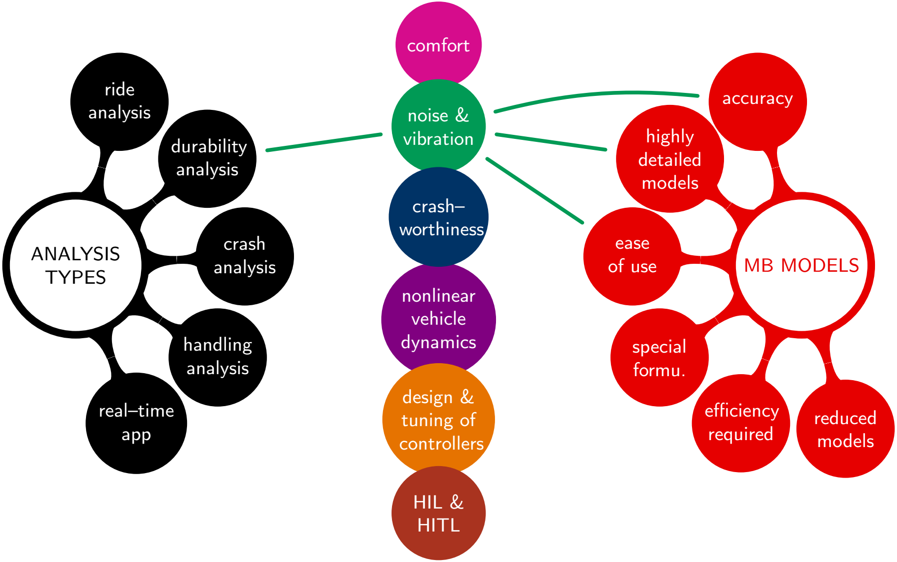

Multibody dynamics analysis in the automotive field.

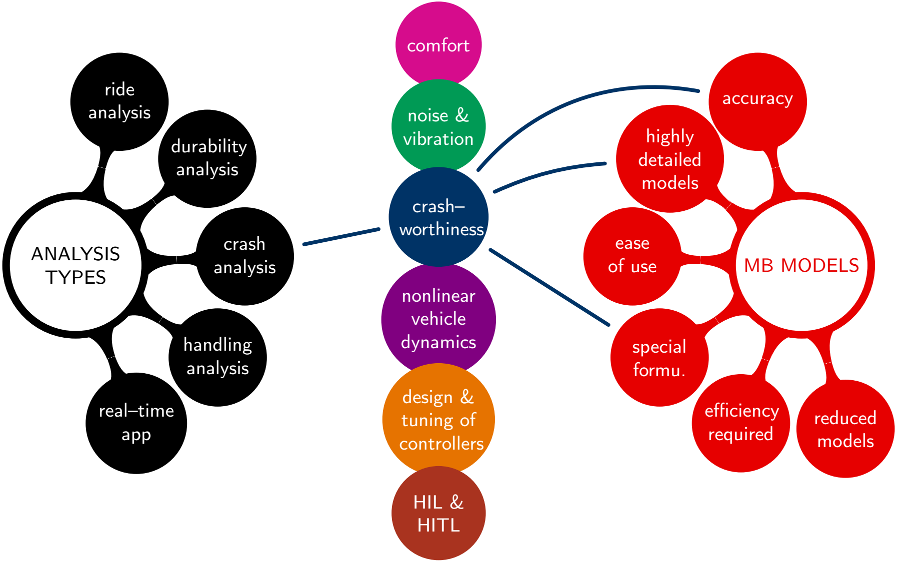

Multibody dynamics analysis in the automotive field.

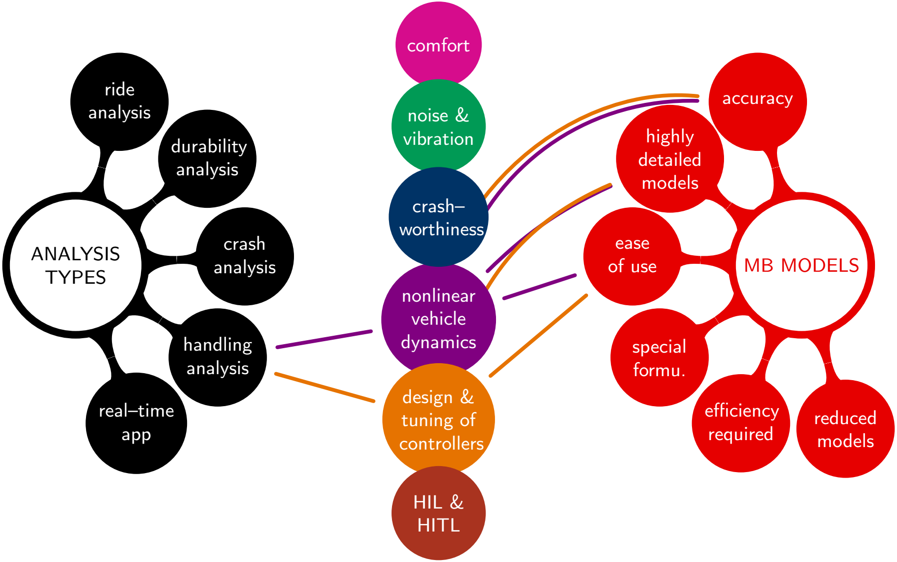

Multibody dynamics analysis in the automotive field.

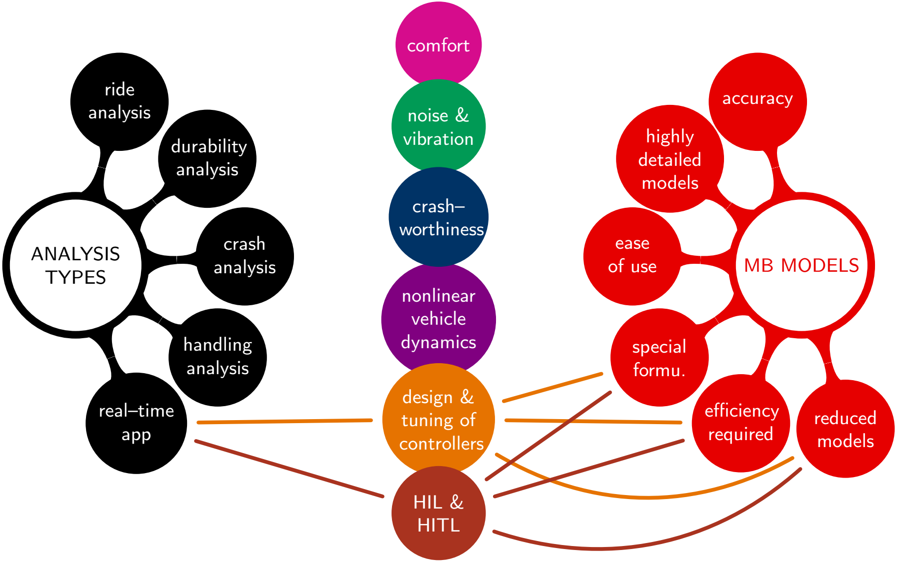

Objectives.

> "Without validation of the vehicle dynamics there is only speculation that a given model accurately predicts a vehicle response"
>
> **A.H. Hoskins and M. El-Gindy, "Technical report: Literature survey on driving simulator validation studies", International Journal of Heavy Vehicle Systems, vol. 13 (3), pp. 241–252, (2006)**

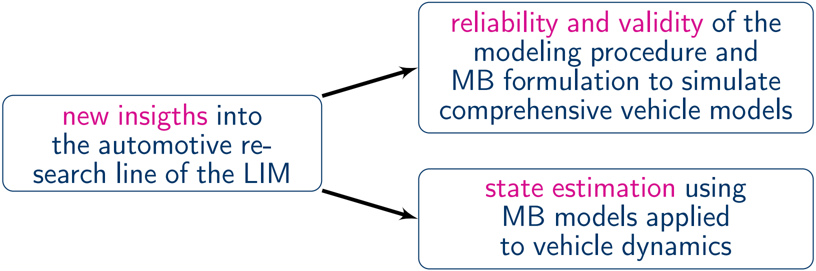

Validation methodology.

- based on the validation methodology developed by the VRTC (Vehicle Research and Test Center) for the NADS (National Advanced Driving Simulator)
- composed of 3 main phases

1 – experimental data collection → **2 – vehicle parameter measurement** → **3 – simulation predictions vs experimental data**

1 – experimental data collection:
- vehicle field testing
- maneuvers → broad range of vehicle operating conditions
- repetitive maneuvers to determine the random uncertainty
- experimental post–processing

2 – vehicle parameter measurement:
- parameter measurements for the MB model and the subsystem models

3 – simulation predictions vs experimental data:
- simulations using the same control inputs that were measured at the 1st phase
- comparisons between the simulation & experimental results

Fig. 5 – NADS bay

Diagram of the iterative validation methodology.

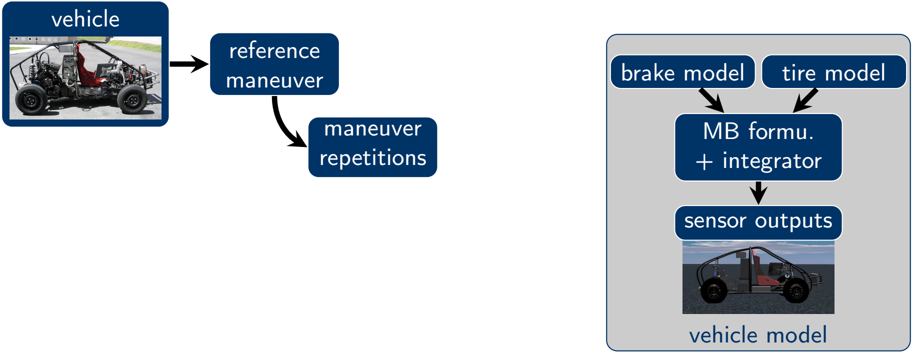

Diagram of the iterative validation methodology.

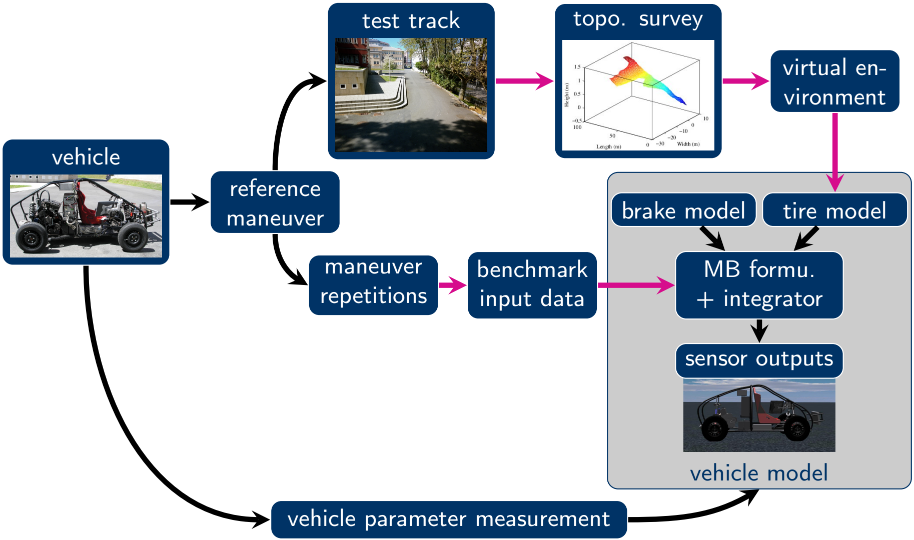

Diagram of the iterative validation methodology.

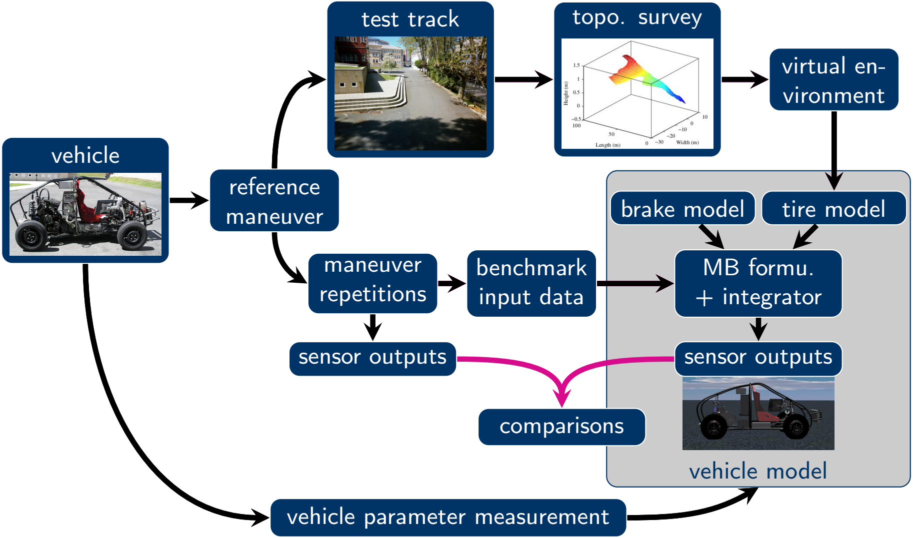

Diagram of the iterative validation methodology.

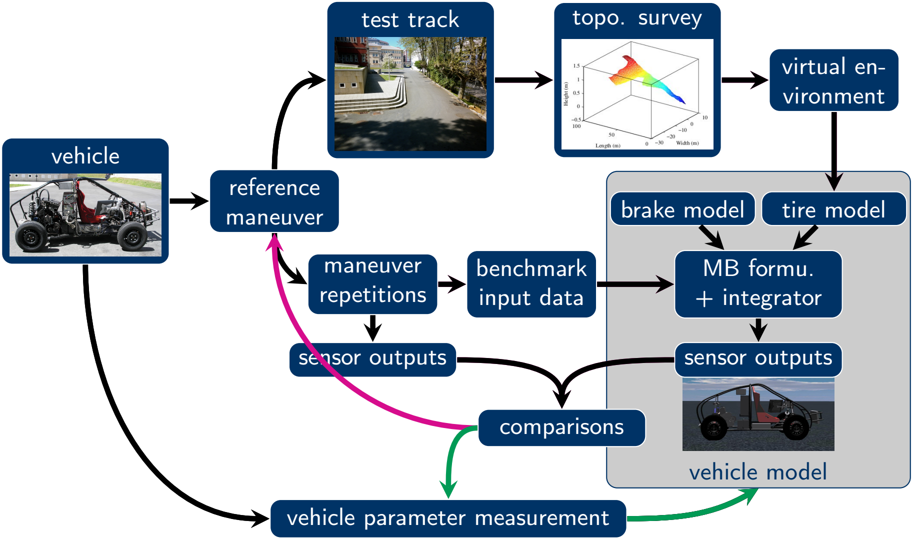

The XBW vehicle prototype.

- self–developed from scratch
- on–board digital acquisition system
- longitudinal and lateral maneuver repetition capability

Mechanical characteristics.

- tubular frame
- internal combustion engine (4 cylinders, 2–barrel carburator)
- automatic gearbox transmission
- front suspension → double wishbone
- rear suspension → MacPherson
- tyres → Michelin E3B1 Energy 155/80 R13

Fig. 6 – Design and manufacturing

Fig. 7 – XBW vehicle prototype

The by–wire systems of the prototype.

- SBW → steer–by–wire
- TBW → throttle–by–wire
- BBW → brake–by–wire

Extra sensors.

Measured magnitudes	Sensors
vehicle accelerations (X,Y,Z)	accelerometers (m/s^2)
vehicle angular rates (X,Y,Z)	gyroscopes (rad/s)
vehicle orientation angles	inclinometers (rad)
wheel rotation angles	hall–effect sensor (rad)
brake line pressure	pressure sensor (kPa)
steering wheel and steer angles	encoders (rad)
engine speed	hall–effect sensors (rad/s)
steering torque	inline torque sensor (Nm)
throttle pedal angle	encoder (rad)
rear wheel torque	wheel torque sensor (Nm)

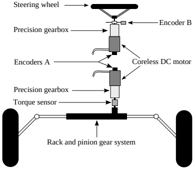

Fig. 8 – Steer–by–wire system

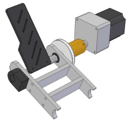
Fig. 9 – Throttle–by–wire system

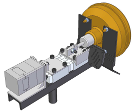
Fig. 10 – Brake–by–wire system

Driver's force feedback of the SBW.

- objective → accurate torque feedback to the driver
- problem → flexibility, backlash & friction
- solution → highly accurate model of the assembly *amplifier–motor–gearbox*
- future work → model based torque controller

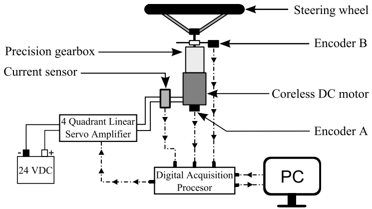

Fig. 12 – Steering wheel system

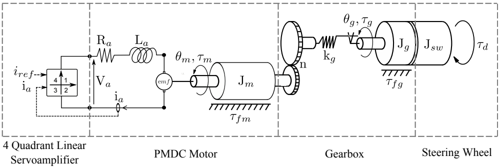

Fig. 11 – Scheme of the modeling

Fig. 13 – CAD model of the steering wheel system

7 repetitions of a low speed straight–line maneuver.

- total distance = 63.5 m
- max speed = 23 km/h

6 repetitions of a low–speed J–turn maneuver.

- total distance = 59.6 m
- max speed = 18 km/h

Vehicle modeling.

- Type of coordinates : natural + some relative coordinates (angles & distances)
- MB formulation : index–3 augmented Lagrangian formulation with mass–damping–stiffness–orthogonal projections
- Bodies / Variables : 18 → all the vehicle bodies / 168 → points and vectors
- Steering : kinematically guided
- Forces : gravity forces, tire forces, engine torque, brake torques
- Degrees of freedom : 14 → suspension systems (4)
  chassis (6)
  wheels (4)

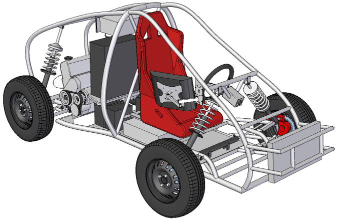

Fig. 14 – CAD model of the prototype

Fig. 15 – Points & vectors of the MB model

Efficient MB formulation developed and used at LIM.

- index–3 augmented Lagrangian formulation with mass–damping–stiffness–orthogonal projections
- integration → the trapezoidal rule and the Newton–Raphson method

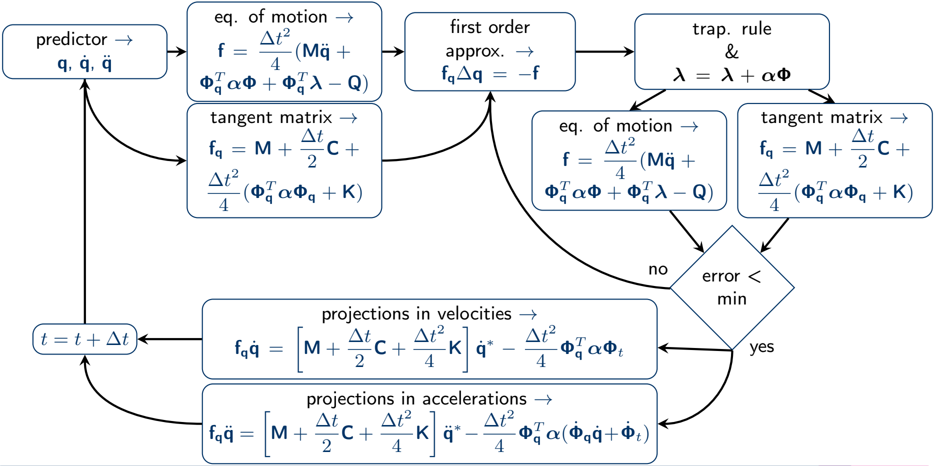

Tire model.

- part of the empirical and physical *TMeasy* model
- first–order dynamics → longitudinal and lateral deflections
- transition to stand–still → stick–slip behavior
- tire curves → linearized model

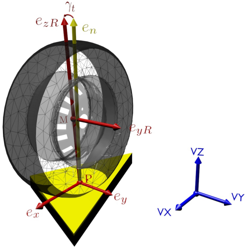

Fig. 16 – Points & vectors for the tire modeling

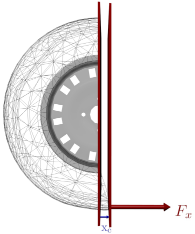

Fig. 17 – Longitudinal deformation of the tire

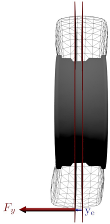

Fig. 18 – Lateral deformation of the tire

Road profile.

- topographical survey of the test track with a total station
- 300 points for a track of 80 meters long
- interpolation of the scattered points
- Delaunay triangulation → mesh of triangles for the collision detection

Fig. 19 – Total station used for the topographical survey

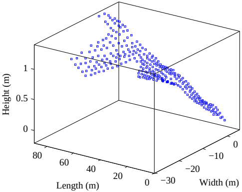

Fig. 20 – 3D scattered points

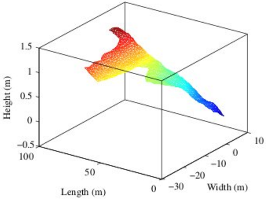

Fig. 21 – 3D model of the test track

Collision detection.

- tire normal force → function of the inter–penetration of the stepped triangles of the ground mesh
- 4 spheres for the collision geometry of the tires

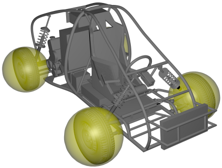

Fig. 22 – 3D model of the test track

Simulation environment.

- realistic graphical environment of the campus
  - self–developed 3D environment
  - open–source 3D graphics toolkit (C++)
- inclusion of the topographical survey of the test track

MB model inputs.

- averaging of the experimental data

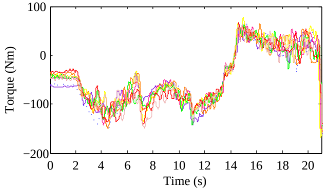

Fig. 23 – Repetitions (wheel torque)

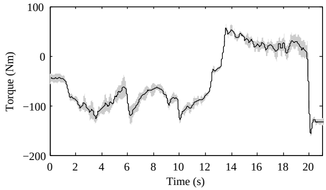

Fig. 24 – Mean and CI (wheel torque)

Confidence intervals.

- assumption → the uncertainty follows a normal distribution
- small number of samples → Student's t distribution

C.I. bounds: $\bar{x} \pm t^{n-1}_{(1-\alpha/2)} \cdot \frac{S}{\sqrt{n}}$

sample mean → $\bar{x} = \frac{1}{n}\sum_{i=1}^{n} x_i$

sample variance → $S^2 = \frac{1}{(n-1)}\sum_{i=1}^{n}(x_i - \bar{x})^2$

$(1-\alpha/2)$ critical value for the t distribution with $(n-1)$ degrees of freedom

Simulation of the low speed straight–line maneuver.

- MB model inputs → averaged experimental data
- road profile → topographical survey

Validation results for the low speed straight–line maneuver.

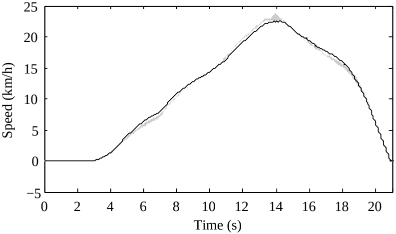

Fig. 25 – Left front wheel speed

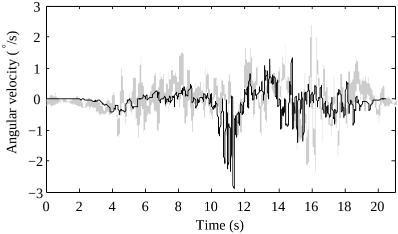

Fig. 26 – Roll rate of the chassis

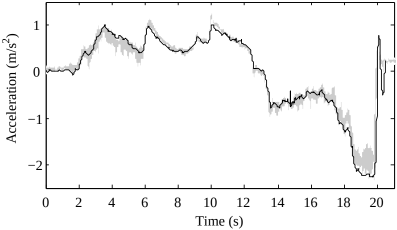

Fig. 27 – Longitudinal acceleration of the chassis

Simulation of the low–speed J–turn maneuver.

- MB model inputs → averaged experimental data
- road profile → topographical survey

Validation results for the low speed J–turn maneuver.

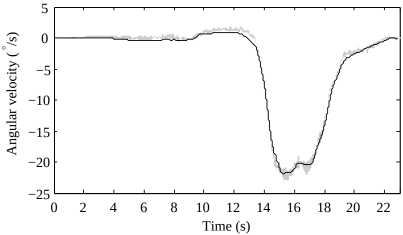

Fig. 28 – Yaw rate of the chassis

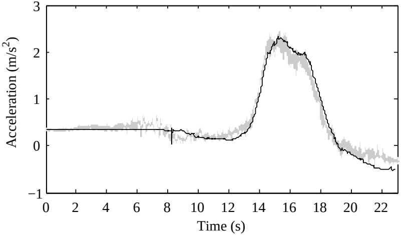

Fig. 29 – Lateral acceleration of the chassis

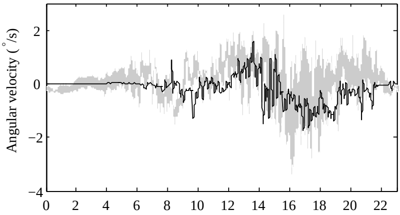

Fig. 30 – Roll rate of the chassis

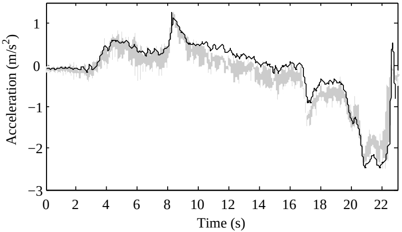

Fig. 31 – Longitudinal acceleration of the chassis

Model running in real–time with the same inputs

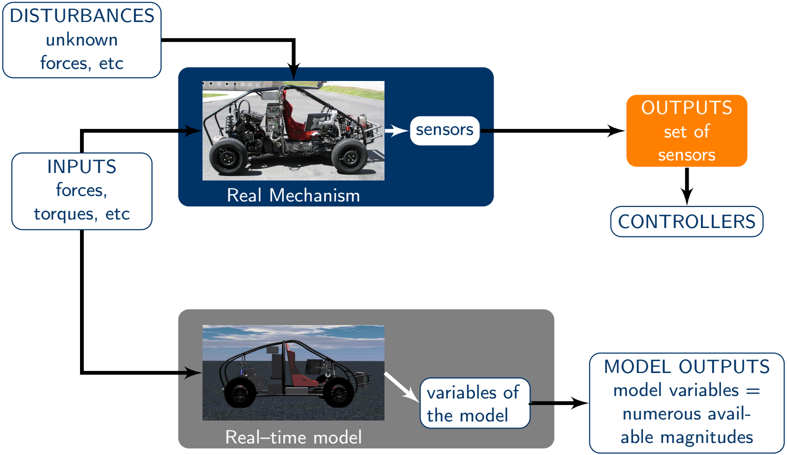

Model running in real–time with the same inputs

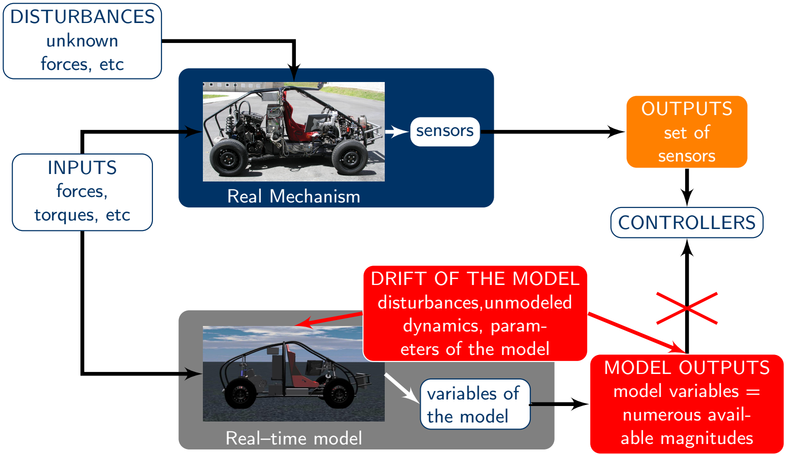

State observers for mechanical systems based on Kalman filters

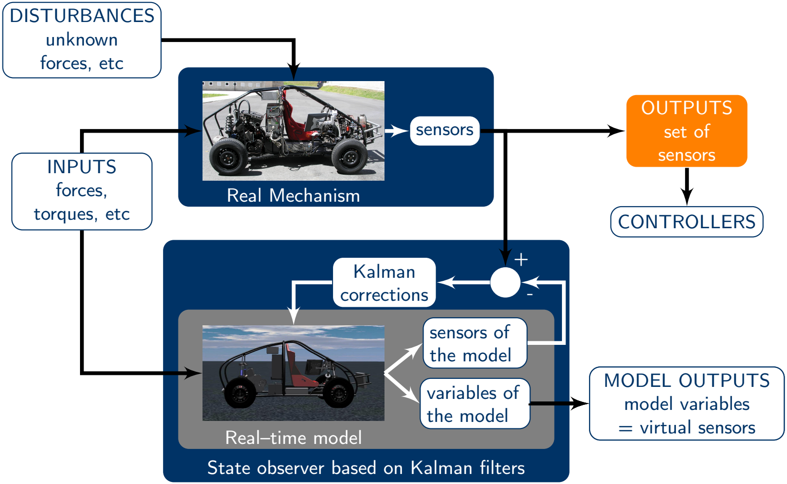

State observers for mechanical systems based on Kalman filters

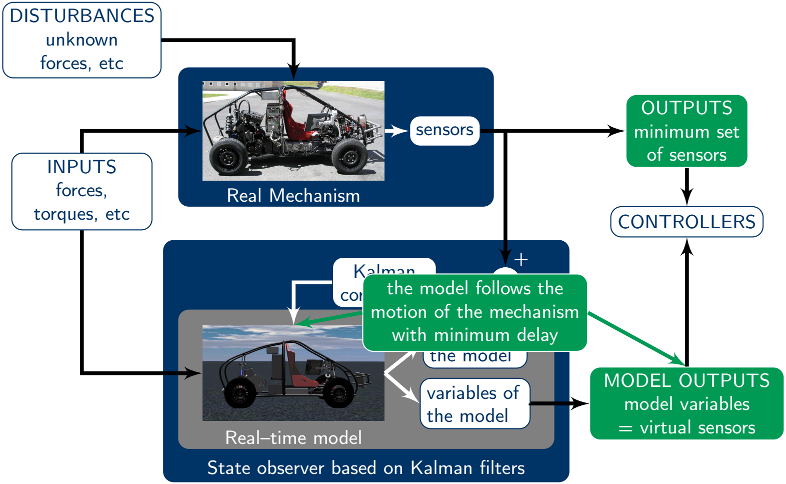

State estimation in mechanical systems.

- Advantages

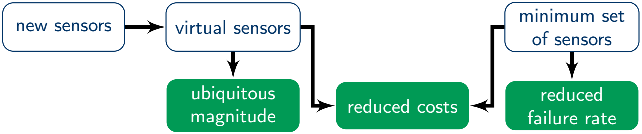

The more detailed the model is, the more it provides information about the motion of the mechanism

- Past researches
  - Kalman filter + linear mechanical systems
  - linearized Kalman filter + nonlinear mechanical systems

} lack of generality
linear models
simple nonlinear models

First implementations using a 4–bar linkage and a VW Passat.

- Recent researches at the LIM
  - extended Kalman filter + real–time MB models } general approach, complex nonlinear models

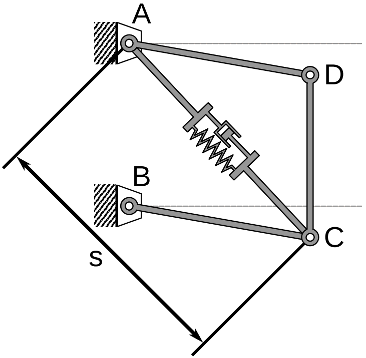

Fig. 32 – 4–bar linkage

Fig. 33 – VW passat & model & state observer w/ MB model

Description.

- simple mechanism: 5–bar linkage → 2 DOFs
- mechanism parameters → experimental measurements
- parameters of the sensors → characteristics from off–the–shelf sensors

MB Modeling.

- natural coordinates (8 variables, 6 constraints, 2 DOFs)
- MB formulations
  - independent coordinates → projection matrix–R method
  - dependent coordinates → penalty formulation
- simulation of the real mechanism for comprehensive comparisons
- known errors between the real mechanism and its MB model → lengths, masses, inertias. . .

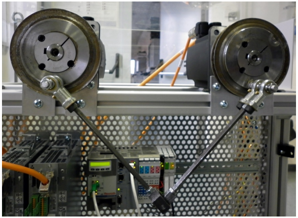

Fig. 34 – 5–bar linkage image

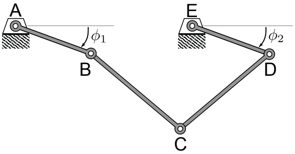

Fig. 35 – 5–bar linkage modeling scheme

Free motion simulation.

- Drift of the model due to errors in the parameters of the model

real mechanism
(matrix–R, trap. rule)

model
(matrix–R, trap. rule)

Comparison of NL Kalman filters.

		SPKF	
	EKF	UKF	SSUKF
What is it?	*de facto* NL Kalman filter	recent NL Kalman filters	
Why to use it ?	efficiency	accuracy and easy implementation	
Which form ?	continuous	discrete	
How does it work ?	state estimates → propagation through NL system. mean and state estimation uncertainty → propagation through linearization	state estimates → propagation through NL system. mean and state estimation uncertainty → propagation of sigma–points through the NL system	
Assumptions	additive white Gaussian noises		

System dynamics

$$\dot{\mathbf{x}}(t) = \mathbf{f}(\mathbf{x}(t)) + \boldsymbol{w}(t)$$

← first order differential equations with independent states

$$\mathbf{x}_{k+1} = \phi_k(\mathbf{x}_k) + \boldsymbol{w}_k$$

← nonlinear difference equations with independent states

The extended Kalman filter – EKF.

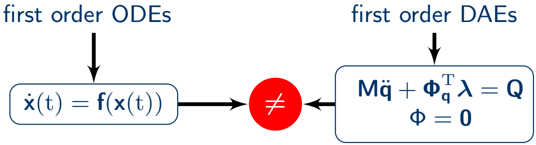

The extended Kalman filter – EKF.

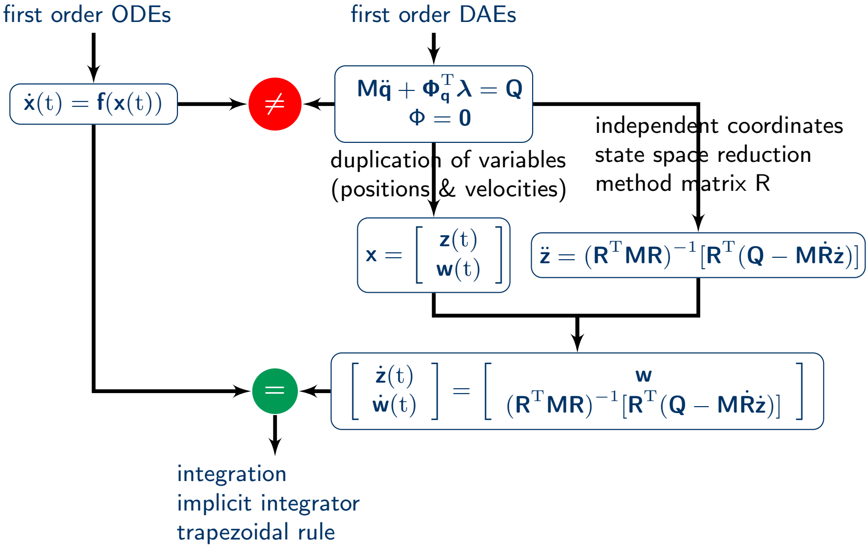

The extended Kalman filter – EKF.

state estimates

$$\dot{\hat{\mathbf{x}}}(t) = \mathbf{f}(\hat{\mathbf{x}}(t), t) + \bar{\mathbf{K}}[\mathbf{y}(t) - \hat{\mathbf{y}}(t)]$$

Kalman gain

$$\bar{\mathbf{K}}(t) = \mathbf{P}(t)\mathbf{H}^{[1]\mathrm{T}}(t)\boldsymbol{\mathcal{R}}(t)$$

Riccati equation

$$\dot{\mathbf{P}}(t) = \mathbf{F}^{[1]}\mathbf{P}(t) + \mathbf{P}(T)\mathbf{F}^{[1]\mathrm{T}} + \mathbf{G}\mathbf{Q}(t)\mathbf{G}^{\mathrm{T}} - \bar{\mathbf{K}}\boldsymbol{\mathcal{R}}(t)\bar{\mathbf{K}}$$

linear approximations

$$\mathbf{F}^{[1]}(t) \simeq \frac{\partial \mathbf{f}(\mathbf{x}, t)}{\partial \mathbf{x}} \qquad \mathbf{H}^{[1]}(t) \simeq \frac{\partial \mathbf{h}(\mathbf{x}, t)}{\partial \mathbf{x}}$$

$$\mathbf{F}^{[1]}(t) = \begin{bmatrix} \mathbf{0} & \mathbf{I} \\ \dfrac{\partial(\bar{\mathbf{M}}^{-1}\bar{\mathbf{Q}})}{\partial \mathbf{z}} & \dfrac{\partial(\bar{\mathbf{M}}^{-1}\bar{\mathbf{Q}})}{\partial \mathbf{w}} \end{bmatrix} \simeq \begin{bmatrix} \mathbf{0} & \mathbf{I} \\ -\bar{\mathbf{M}}^{-1}\mathbf{R}^{\mathrm{T}}(\mathbf{K}\mathbf{R} + 2\mathbf{M}\mathbf{R}_{\mathbf{q}}\mathbf{R}\dot{\mathbf{w}}) & -\bar{\mathbf{M}}^{-1}\mathbf{R}^{\mathrm{T}}(\mathbf{C}\mathbf{R} + \mathbf{M}\dot{\mathbf{R}}) \end{bmatrix}$$

The unscented Kalman filter – UKF.

nonlinear recurrences
with independent states

$$\mathbf{x}_{\mathrm{k}+1} = \phi_{\mathrm{k}}(\mathbf{x}_{\mathrm{k}})$$

$\neq$

first order DAEs

$$\mathbf{M}\ddot{\mathbf{q}} + \mathbf{\Phi}_{\mathbf{q}}^{\mathrm{T}}\boldsymbol{\lambda} = \mathbf{Q}$$
$$\mathbf{\Phi} = \mathbf{0}$$

The unscented Kalman filter – UKF.

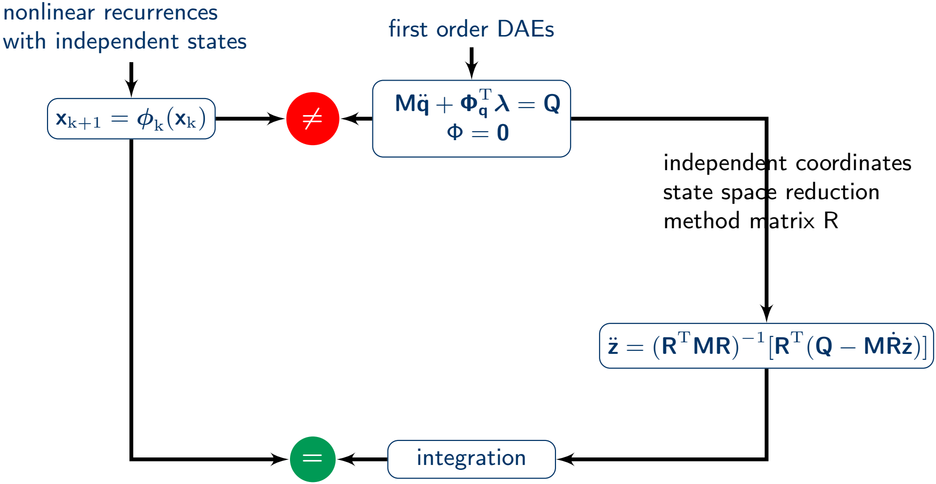

The unscented Kalman filter – UKF.

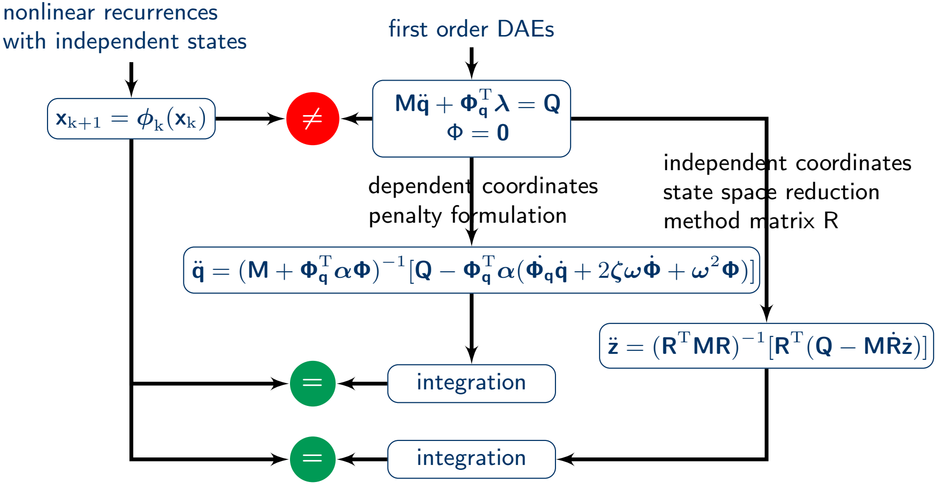

The unscented Kalman filter – UKF.

time–update equations (always executed)

$$\hat{\mathbf{x}}_k^- = \sum_{i=0}^{2L} w_i^m \boldsymbol{\chi}_{i,k|k-1}$$

$$\boldsymbol{\chi}_{k|k-1} = \phi_{k-1}(\boldsymbol{\chi}_{k-1})$$

$$\boldsymbol{\chi}_{i,k-1} = \begin{cases} \hat{\mathbf{x}}_{k-1} \\ \hat{\mathbf{x}}_{k-1} + \gamma \left(\sqrt{\mathbf{P}_{k-1}}\right)_i \\ \hat{\mathbf{x}}_{k-1} - \gamma \left(\sqrt{\mathbf{P}_{k-1}}\right)_i \end{cases}$$

$$\mathbf{P}_{\mathbf{x}_k}^- = \sum_{i=0}^{2L} \omega_i^c (\boldsymbol{\chi}_{k|k-1} - \hat{\mathbf{x}}_k^-)(\boldsymbol{\chi}_{k|k-1} - \hat{\mathbf{x}}_k^-)^T$$

measurement–update equations (executed if information from the sensors is available)

$$\hat{\mathbf{x}}_k = \hat{\mathbf{x}}_k^- + \bar{\mathbf{K}}_k(\mathbf{y}_k - \hat{\mathbf{y}}_k^-)$$

$$\bar{\mathbf{K}}_k = \mathbf{P}_{\mathbf{x}_k\mathbf{y}_k}\mathbf{P}_{\tilde{\mathbf{y}}_k}^{-1}$$

$$\hat{\mathbf{y}}_k^- = \sum_{i=0}^{2L} \omega_i^m \boldsymbol{\mathcal{Y}}_{i,k|k-1}$$

$$\boldsymbol{\mathcal{Y}}_{k|k-1} = \mathbf{h}_k(\boldsymbol{\chi}_{k|k-1})$$

$$\mathbf{P}_{\mathbf{x}_k} = \mathbf{P}_{\mathbf{x}_k}^- - \bar{\mathbf{K}}_k\mathbf{P}_{\tilde{\mathbf{y}}_k}\bar{\mathbf{K}}_k^T$$

The unscented Kalman filter – UKF.

time–update equations (always executed)

$$\hat{\mathbf{x}}_k^- = \sum_{i=0}^{2L} w_i^m \boldsymbol{\chi}_{i,k|k-1}$$

$$\boldsymbol{\chi}_{k|k-1} = \phi_{k-1}(\boldsymbol{\chi}_{k-1})$$

$$\boldsymbol{\chi}_{i,k-1} = \begin{cases} \hat{\mathbf{x}}_{k-1} \\ \hat{\mathbf{x}}_{k-1} + \gamma\left(\sqrt{\mathbf{P}_{k-1}}\right)_i \\ \hat{\mathbf{x}}_{k-1} - \gamma\left(\sqrt{\mathbf{P}_{k-1}}\right)_i \end{cases}$$

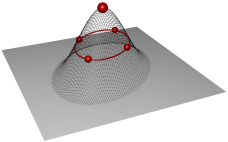

Fig. 36 – Set of sigma–points (2 dim. GR variable)

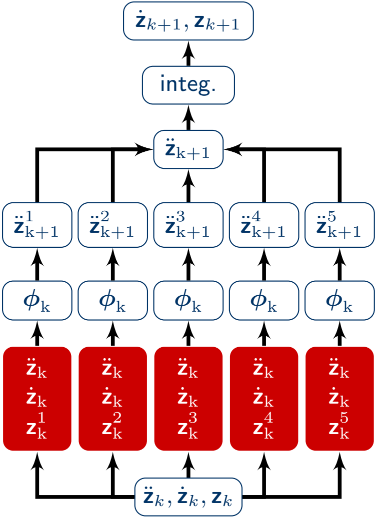

The spherical simplex UKF.

- same equations as for the UKF
- reduced set of sigma–points
  - UKF $\rightarrow$ (2L+1) sigma–points
  - SSUKF $\rightarrow$ (L+2) sigma–points
  - equations of the reduced set of sigma–points

$$\boldsymbol{\chi}_i^j = \begin{cases} \begin{bmatrix}\boldsymbol{\chi}_0^{j-1}\\ \mathbf{0}\end{bmatrix} & \text{for } i=0 \\ \begin{bmatrix}\boldsymbol{\chi}_i^{j-1}\\ -\dfrac{1}{\sqrt{j(j+1)w_1}}\end{bmatrix} & \text{for } i=1,\dots,j \\ \begin{bmatrix}\mathbf{0}_{j-1}\\ \dfrac{1}{\sqrt{j(j+1)w_1}}\end{bmatrix} & \text{for } i=j+1\end{cases}$$

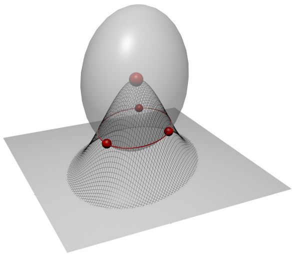

Fig. 37 – Reduced set of sigma–points (2 dim. GR variable

Free motion simulation.

- Drift of the model due to errors in the parameters of the model
- The observers estimate correctly the motion of the real mechanism

- real mechanism (matrix–R, trap. rule)
- model (matrix–R, trap. rule)
- EKF (matrix–R, trap. rule)
- UKF (matrix–R, trap. rule)
- SSUKF (matrix–R, trap. rule)
- SSUKF (matrix–R, RK2)
- SSUKF (penal, RK2)

Performance comparisons of the filters → efficiency vs RMSE.

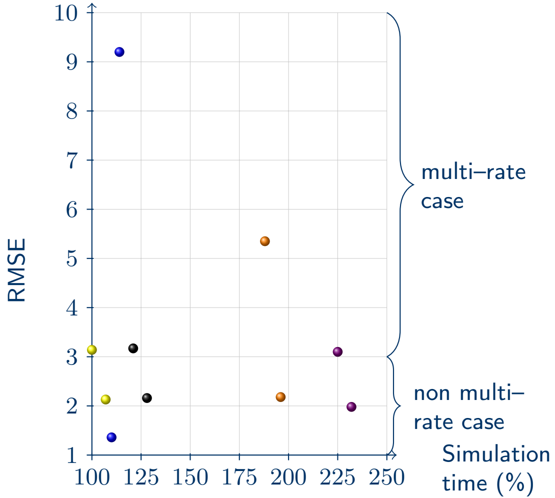

- non multi–rate
  $\Delta t_{integ} = 2ms$
  $\Delta t_{sensors} = 2ms$
- multi–rate
  $\Delta t_{integ} = 2ms$
  $\Delta t_{sensors} = 6ms$

- EKF (matrix–R, trap. rule)
- UKF (matrix–R, trap. rule)
- SSUKF (matrix–R, trap. rule)
- SSUKF (matrix–R, RK2)
- SSUKF (penal, RK2)

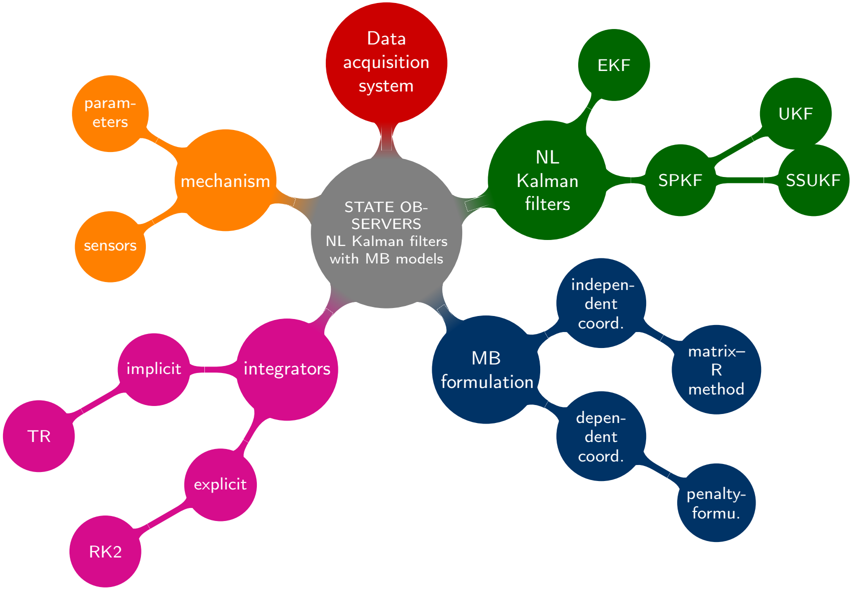
Data acquisition system
param- eters
mechanism
sensors
EKF
UKF
NL Kalman filters
SPKF
SSUKF
STATE OB- SERVERS NL Kalman filters with MB models
indepen- dent coord.
matrix–R method
MB formulation
depen- dent coord.
penalty- formu.
implicit
integrators
TR
explicit
RK2

Pros & Cons.

- EKF
  - Pros → most efficient filter with independent coordinates
  - Cons → involved and error–prone calculation of the Jacobian, not suitable to employ with dependent coordinates, not multi–rate

- SPKFs
  - Pros → easiest implementation, possible use of dependent coordinates, highest accuracy
  - Cons → high computational cost due to the sigma–points

Vehicle field testing.

1. X-by-wire vehicle prototype from scratch
2. highly detailed model of the driver's force feedback system
3. repetitions of 2 reference manoeuvres in the campus

Vehicle modeling and simulation environment.

1. real-time 14 DOFs MB model
2. modelling of subsystems $\rightarrow$ tire, brake
3. topographical survey of the test track
4. realistic 3D simulation environment

Validation results.

1. confidence intervals for the experimental data
2. simulation of the test manoeuvres using the experimental data
3. evaluation of the accuracy of the MB model

State observers.

1. use of MB models with the extended Kalman filter
2. application to a 4–bar linkage and a VW Passat
3. use of MB models with SPKFs filters
4. implementation using a 5–bar linkage

Future research.

1. field testing
   - manoeuvres at higher speeds $\rightarrow$ new test track
   - GPS RTK for real–time positioning of the vehicle
2. vehicle modelling and simulation environment
   - better characterization of the tire curves
   - Human–In–The–Loop simulation using experimental inputs
3. state observers
   - EKF in discrete form
   - research on the observability of MB models
   - tests of the UKF/SSUKF with more complex mechanisms
   - implementation using the MB model of the XBW prototype

Congress papers.

[1] J. Cuadrado, D. Dopico, J. A. Pérez, and R. Pastorino. Influence of the sensored magnitude in the performance of observers based on multibody models and the extended Kalman filter. In *Proceedings of the Multibody Dynamics ECCOMAS Thematic Conference*, Warsaw, Poland, June 2009.

[2] R. Pastorino, M. A. Naya, J. A. Pérez, and J. Cuadrado. X–by–wire vehicle prototype: a steer–by–wire system with geared PM coreless motors. In *Proceedings of the 7th EUROMECH Solid Mechanics Conference*, Lisbon, Portugal, September 2009.

[3] J. Cuadrado, D. Dopico, M. A. Naya, and R. Pastorino. Automotive observers based on multibody models and the extended Kalman filter. In *The 1st Joint International Conference on Multibody System Dynamics*, Lappeenranta, Finland, May 2010.

[4] R. Pastorino, M. A. Naya, A. Luaces, and J. Cuadrado. X–by–wire vehicle prototype: automatic driving maneuver implementation for real–time MBS model validation. In *Proceedings of the 515th EUROMECH Colloquium*, Blagoevgrad, Bulgaria, 2010.

[5] R. Pastorino. La simulation des systèmes multicorps dans l'automobile. *Interface, revue des ingénieurs des INSA de Lyon, Rennes, Rouen, Toulouse*, (111):22, 3ème et 4ème trimestre 2011.

[6] R. Pastorino, D. Dopico, E. Sanjurjo, and M. A. Naya. Validation of a multibody model for an x–by–wire vehicle prototype through field testing. In *Proceedings of the ECCOMAS Thematic Conference Multibody Dynamics 2011*, Brussels, Belgium, 2011.

[7] R. Pastorino, M. A. Naya, A. Luaces, and J. Cuadrado. X–by–wire vehicle prototype : a tool for research on real–time vehicle multibody models. In *Proceedings of the 13th EAEC European Automotive Congress*, Valencia, Spain, June 2011.

[8] R. Pastorino, D. Richiedei, J. Cuadrado, and A. Trevisani. State estimation using multibody models and nonlinear Kalman filters. In *The 2nd Joint International Conference on Multibody Systems Dynamics*, Stuttgart, Germany, May 2012.

[9] R. Pastorino, D. Richiedei, J. Cuadrado, and A. Trevisani. State estimation using multibody models and unscented Kalman filters. In *Proceedings of the 524th EUROMECH Colloquium*, Enschede, Netherlands, 2012.

[10] E. Sanjurjo, R. Pastorino, D. Dopico, and M. A. Naya. Validación experimental de un modelo multicuerpo de un prototipo de vehículo automatizado. In *XIX Congreso Nacional de Ingeniería Mecánica (to be presented)*, Castellón, Spain, Nov. 2012.

Journal papers.

[1] J. Cuadrado, D. Dopico, J. A. Pérez, and R. Pastorino. Automotive observers based on multibody models and the Extended Kalman Filter. *Multibody System Dynamics*, 27(1):3–19, 2011.

[2] R. Pastorino, M. A. Naya, J. A . Pérez, and J. Cuadrado. Geared PM coreless motor modelling for driver's force feedback in steer–by–wire systems. *Mechatronics*, 21(6):1043–1054, 2011.

Journal papers in preparation.

[1] R. Pastorino, M.A. Naya, and J. Cuadrado. Experimental validation of a multibody model for a vehicle prototype. *Vehicle System Dynamics*, 2012.

[2] R. Pastorino, D. Richiedei, J. Cuadrado, and A. Trevisani. State estimation using multibody models and nonlinear kalman filters. *Proceedings of the Institution of Mechanical Engineers, Part K: Journal of Multi–body Dynamics*, 2012.

Acknowledgments.

- Spanish Ministry of Science and Innovation – Grant TRA2009–09314 (ERDF funds)